THE ASTROPHYSICAL JOURNAL, 215:62–73, 1977 July 1

FAINT PHOTOMETRY IN M15: THE INTRINSIC WIDTH OF THE MAIN SEQUENCE, THE LUMINOSITY FUNCTION, AND THE DENSITY GRADIENT OF FAINT FIELD STARS

ALLAN SANDAGE AND BASIL KATEM
Hale Observatories, Carnegie Institution of Washington, California Institute of Technology
Received 1976 October 1

ABSTRACT

Photometry of ~350 stars between $18.7 < V \leqslant 22$ in an area of 22 square arcmin located 8′ north of the globular cluster M15 shows a main sequence whose observed width is due almost entirely to the known errors of measurement. The intrinsic width in color is smaller than $\sigma[\delta(B - V)] \leqslant 0.03$ mag, or equivalently $\sigma(\delta V) \leqslant 0.2$ in magnitude. These limits put restrictions on any inhomogeneity in the distribution of helium abundance to be $\sigma(\delta Y) < \pm 0.08$, if $\langle Y \rangle \approx 0.3$. A limit on the permissible distribution of differences in the interior metal abundance between the member stars, obtained from the narrowness of the M15 giant-subgiant branch of $\sigma[\delta(B - V)] < 0.01$ mag, is $\sigma(\delta Z/Z) < \pm 0.16$. These upper limits to both X and Y show that the M15 protocloud could not have been significantly enriched in a progressive way during its collapse.

The main-sequence luminosity function rises at the rate $d \log \varphi(V)/dV \approx \pm 0.35$ between $M_V = +3.5$ and 5.5, but may flatten from $M_V > 5.5$ to the plate limit.

The number of foreground field dwarfs between $M_V = +8$ and $+12$ is so small in the M15 area as to require a steep density gradient of $d \log D(z)/dz \approx -1.1$ (z in kpc), similar to that required to explain Becker's photometry of very faint stars in SA 57, and similar to Weistrop's results in the range $300 \leqslant z \leqslant 2000$ pc. This gradient is so much steeper than that for RR Lyrae stars (~ -0.2) that it suggests that the bulk of the red stars we observe between $V = 19$ and 22 are not halo Population II dwarfs, but rather are an extension of the old disk to $z \approx 2$ kpc. The results can be explained if the disk and halo populations coexist at that height, with the disk density outnumbering the halo by a large factor below $z \approx 2$ kpc, and the halo dominating beyond $z \geqslant 3$ kpc.

Subject headings: clusters: globular — luminosity function — stars: abundances — stars: stellar statistics

I. INTRODUCTION

Photographic photometry of 343 stars between $18.7 < V \leqslant 22$ in M15 has been done in an area of 22 arcmin^2 in an outer zone of the cluster. Five plates in each of two colors (B and V) taken with the Hale 5 m reflector were measured with an iris photometer relative to a 54-star standard sequence located ~8′ north of the cluster center.

The original purpose was to search for gaps in the upper evolved main sequence near $M_V \approx +5$ just below the turnoff luminosity, analogous to the hydrogen exhaustion gap in M67, NGC 188, and younger clusters. No gap is expected in globular clusters because the p-p chain presumably dominates over the CNO cycle, and a convective core should be absent. But it seemed interesting to test the point because early models of the stars in NGC 188 predicted no gap either, yet it may exist (Eggen and Sandage 1969).

As a control, similar photometry was done in M92 on the supposition that if a gap was found in M15 and if it were real, then it should also occur in M92 at about the same place because the metal abundance and the age of M15 and M92 are similar. The photometry of M92 will be reported later.

Unfortunately, the question of the gap remains unanswered by the work, but the faint photometry in M15 proved useful for other purposes such as (1) study of the initial chemical homogeneity of the member stars, (2) the main-sequence luminosity function to $M_V \approx +6.5$, and (3) the density gradient perpendicular to the plane for faint field dwarfs near the base of the galactic halo.

The first problem of the chemical homogeneity has recently become a major concern because of (1) Zinn's (1973*b*) discovery of different chemical compositions for stars along the asymptotic giant branch (AGB) in M92, with subsequent work by Zinn (1973*a*), Mallia (1975, 1976), and Norris and Zinn (1976) on stars on the AGB and the giant branch of many other clusters such as M5, M13, M15, NGC 6397, and ω Cen, (2) the appreciable intrinsic width of the giant branch in ω Cen (Geyer 1967; Cannon and Stobie 1973; Norris and Bessell 1975; Bessell and Norris 1976), and (3) the variation of ΔS among the RR Lyrae stars in ω Cen (Freeman and Rodgers 1975; Butler 1976). Norris and Bessell, following Zinn,

argue that the width of the giant branch in ω Cen, and the variation of the CH abundance (G band) from star to star on the AGB in many clusters suggest mixing onto the surface of the products of nucleosynthesis, either in the He core flash that terminates the giant branch on the first run-up, or in the subsequent He shell ignitions along the AGB. On the other hand, Freeman and Rodgers argue that variations in ΔS among RR Lyrae stars in ω Cen probably cannot be produced by such mixing, and hence that the likely cause is an initial chemical inhomogeneity due to spotty enrichment in space and time within the collapsing protocluster.

In principle, a decision between these two possibilities can be made if we know the intrinsic width of the main sequence and of the giant branch at the level of the horizontal branch, since each is sensitive to variations of the chemical composition. Bessell and Norris argue that the observed narrowness of the giant branch in M15 does not permit initial abundance variations that affect large numbers of the stars. We can also argue the point in the next sections (§§ III, IV) using the observed and inferred intrinsic width of the M15 main sequence, which depends on the chemical homogeneity of the member stars.

The second problem concerns the faint end of the luminosity function. Hints from both observation and theory have suggested in the past that the faint end of the main sequence in globular clusters may be largely missing, due to a variety of dynamical processes, or at least depleted relative to the birthrate function fainter than $M_V \approx +6$. A decline in the slope of the differential luminosity function was claimed in M3 between $M_V = 4.5$ and 6 from early counts (which should be repeated) in that cluster (Sandage 1954, corrected in 1957), and an actual turnover has recently been reported in M92 (van den Bergh 1975), where the photometry is probably more secure than in M3. The faint M15 photometry here permits beginning of a third study of the problem in § V.

A related question is the frequency of faint main-sequence dwarfs between $M_V \approx +8$ and $M_V \approx +12$ at the galactic pole. The problem concerns the birthrate function and its dependence on height above the plane. The number of faint red *field* stars in the M15 photometry, discussed in § VI, gives a clue to the polar density function $D(z)$, as does a more direct calculation from Becker's (1970) photometry in SA 57 that reaches $V \approx 22$.

II. THE PHOTOMETRY

The plates were calibrated using the smoothed (photographic) sequence north of M15 that is based on photoelectric measurements (Sandage 1970, Table 5 and Fig. 8). Most stars in an annular sector between $r = 6'.8$ and $9'.8$ radius from the center were measured, and are identified in Figure 1 (Plate 4). The region is divided into 10 smaller areas designated by sector numbers (I and II) and bin numbers (W1–W5). A few other stars, all standards, are identified in sector III, but no program stars were measured there. All the calibration standards are circled in Figure 1.

The mean values from measurement of the five plates in each color (103a-O + GG13; 103a-D + GG11), corrected for field errors as described below, are listed in Table 1, ordered by sector and bin numbers.

The first part of the table gives values for the standard stars, as read back through the calibration curves. Comparison with the adopted sequence shows good agreement at all magnitudes, but it must be emphasized that the range of color among the standards is so small that no adequate test of the color equation between the photographic and the true BV system can be made. The data are left on the natural system of the plates. Hence, colors for the redder stars ($B - V \gtrsim 1$) in the field are likely to have a systematic difference from the Johnson-Morgan systems, and no very detailed analysis that requires *accurate* colors for them should be made.

The data in Table 1 have been partly adjusted for field errors, depending on position on the plates, by an approximate procedure. The color-magnitude (CM) diagram of the standard stars alone was drawn and compared with the diagrams for each separate bin. It was found that the main sequence (ms) in each diagram was well defined, but some were shifted in $B - V$ relative to that for the standard stars. Shifts in $B - V$, as listed in Table 2, were made to bring all plots into coincidence with the standard diagram.

The shifts are generally systematic with position (the most affected bins are farthest from the plate center), and hence appear to be caused by field errors. *Corrections have been made only to the measured colors to produce Table 1; hence small field errors undoubtedly remain in some of the magnitudes*, and this should be considered if the field is used for tests of area detectors, for example. However, the magnitudes within any given bin are expected to be more homogeneous than those across the entire field.

The errors of measurement for each star in Table 1 were calculated from the residuals of the five plates from the mean. The standard deviations of the error distributions (for a single measurement), binned into half-magnitude intervals, are listed in Table 3. The measuring error increases toward the plate limit as expected, and reaches $\sigma \approx \pm 0.08$ mag at $V = 22$ for a single measurement.

The CM diagram from Table 1 is shown in Figure 2. A well-defined main sequence is evident, together with a sprinkling of redder stars, most of which must be faint foreground dwarfs.

There is a suggestion of a gap in the main sequence at $V = 19.7$ ($M_V \approx +4.4$) at about the relative position of the hydrogen exhaustion gap in NGC 188 and M67, but we are uncertain of its reality. Although a probability for its existence could be calculated following the methods of Aizenman, Demarque, and Miller (1969), we believe that the question would even then not be settled from these data alone, and we have not gone through the formalism. However, it seems

TABLE 1

PHOTOMETRY FROM FIVE PLATES IN EACH COLOR IN THE M15 FIELD

STANDARD STARS

NAME	V	B-V
A11	21.93	0.87
C 1	21.65	0.87
A17	21.60	0.99
A18	21.41	0.77
A 8	21.21	0.71
A 7	21.01	0.63
B 5	20.92	0.66
A 1	20.68	0.65
A16	20.65	0.69
B 7	20.54	0.60
A 5	20.52	0.70
A 6	20.49	0.67
B 8	20.39	0.61
B 3	20.15	0.59
II-W1- 3	19.83	0.47
B 6	19.58	0.51
J	19.54	0.48
I-W3- 5	19.50	0.43
II-W4- 6	19.50	0.49
II-W5- 2	19.45	0.45
II-W2- 5	19.40	0.49
III-W3- 6	19.40	0.48
II-W3- 4	19.36	0.49
II-W5- 1	19.32	0.47
II-W1- 5	19.26	0.43
II-W2- 4	19.25	0.47
II-W4- 3	19.24	0.53
III-W4- 3	19.21	0.52
Q	19.11	0.53
I-W3- 3	19.11	0.48
I-W5- 6	19.11	0.48
III-W2- 2	19.09	0.45
III-W1- 5	19.06	0.50
I-W2- 1	19.02	0.45
III-W5- 4	18.98	0.53
I-W4- 2	18.92	0.50
II-W2- 1	18.92	0.49
II-W2- 2	18.92	0.49
A15	18.91	0.46
II-W2- 6	18.88	0.42
III-W5- 3	18.87	0.51
I-W1- 1	18.86	0.47
III-W5- 1	18.86	0.50
II-W4- 1	18.84	0.53
II-W5- 3	18.84	0.52
III-W5- 2	18.84	0.52
III-W2- 5	18.83	0.43
II-W3- 5	18.82	0.50
E	18.81	0.49
III-W3- 1	18.78	0.50
III-W2- 6	18.76	0.47
I-W5- 0	18.66	0.55
I-W3- 2	18.63	0.54
III-W3- 3	18.33	-0.18

PROGRAM STARS

NAME	V	B-V
I-W1- 1	21.58	0.84
I-W1- 2	20.71	1.07
I-W1- 3	20.98	0.64
I-W1- 4	20.80	1.02
I-W1- 5	21.49	0.73
I-W1- 6	21.32	0.84
I-W1- 7	21.54	0.86
I-W1- 8	20.69	0.67
I-W1- 9	21.08	0.85
I-W1-10	21.64	1.09
I-W1-11	21.21	0.72
I-W1-12	20.63	0.62
I-W1-13	20.21	1.86
I-W1-14	20.82	0.65
I-W1-15	18.64	1.70
I-W1-16	20.03	0.55
I-W1-17	19.24	0.91
I-W1-18	21.09	0.74
I-W1-19	21.85	0.54
I-W1-20	20.85	0.72
I-W1-21	19.54	0.50
I-W1-22	19.28	0.63
I-W1-23	20.21	1.82
I-W1-24	21.24	0.92
I-W1-25	21.18	0.67
I-W2- 1	21.80	1.01
I-W2- 2	21.87	0.85
I-W2- 3	21.41	0.72
I-W2- 4	21.62	0.90
I-W2- 5	19.98	0.57
I-W2- 6	21.08	0.69
I-W2- 7	20.57	0.60
I-W2- 8	20.41	0.55
I-W2- 9	20.32	0.62
I-W2-10	21.69	1.09
I-W2-11	20.62	0.64
I-W2-12	19.62	0.56
I-W2-13	18.71	0.59
I-W2-14	19.48	0.50
I-W2-15	21.74	0.91
I-W2-16	21.63	0.69
I-W2-17	20.81	1.55
I-W2-18	21.73	0.81
I-W2-19	21.54	0.77
I-W2-20	21.72	0.75
I-W2-21	19.98	0.68
I-W2-22	20.14	1.75
I-W2-23	20.16	0.59
I-W2-24	20.89	0.68
I-W2-25	20.24	0.57
I-W2-26	20.92	0.71
I-W2-27	20.72	0.70
I-W3- 1	20.72	0.65
I-W3- 2	21.29	0.75
I-W3- 3	21.52	0.82
I-W3- 4	19.68	1.67
I-W3- 5	21.32	
I-W3- 6	21.51	0.92
I-W3- 7	21.19	0.78
I-W3- 8	20.79	0.64
I-W3- 9	20.39	0.51
I-W3-10	20.99	0.79
I-W3-11	21.87	0.90
I-W3-12	21.46	0.72
I-W3-13	20.66	0.70
I-W3-14	21.90	0.58
I-W3-15	21.37	0.90
I-W3-16	20.84	0.65
I-W3-17	21.30	0.75
I-W3-18	20.36	0.73
I-W3-19	21.37	0.82
I-W3-20	20.45	0.55
I-W3-21	20.74	0.74
I-W3-22	21.00	0.62
I-W3-23	19.98	0.48
I-W3-24	20.53	0.57
I-W3-25	20.49	0.64
I-W3-26	20.26	0.55
I-W3-27	19.63	1.32
I-W3-28	19.65	0.52
I-W3-29	19.66	0.51
I-W3-30	20.50	0.54
I-W4- 1	21.76	0.80
I-W4- 2	21.80	0.91
I-W4- 3	21.60	0.90
I-W4- 4	20.71	0.65
I-W4- 5	20.32	1.02
I-W4- 6	20.64	0.64
I-W4- 7	21.66	0.74
I-W4- 8	21.11	0.83
I-W4- 9	21.42	0.81
I-W4-10	21.33	0.81
I-W4-11	21.87	
I-W4-12	20.89	1.52
I-W4-13	21.46	0.84
I-W4-14	21.50	0.75
I-W4-15	20.59	0.93
I-W4-16	20.80	0.72
I-W4-17	21.93	0.68
I-W4-18	21.36	0.92
I-W4-19	20.80	1.44
I-W4-20	21.50	0.69
I-W4-21	20.57	0.71
I-W4-22	20.05	1.86
I-W4-23	21.19	1.12
I-W4-24	20.75	0.56
I-W4-25	20.92	0.64
I-W4-26	21.11	1.21
I-W4-27	21.28	0.71
I-W4-28	20.47	1.56
I-W4-29	20.66	0.60
I-W4-30	20.27	0.54
I-W4-31	20.95	0.65
I-W4-32	21.16	0.88
I-W4-33	20.83	0.69
I-W4-34	20.69	0.75
I-W4-35	20.98	0.66
I-W4-36	20.64	0.64
I-W4-37	21.06	0.68
I-W5- 1	21.14	0.71
I-W5- 2	20.92	0.73
I-W5- 3	21.81	
I-W5- 4	21.26	0.70
I-W5- 5	21.83	
I-W5- 6	21.94	
I-W5- 7	21.58	0.73
I-W5- 8	21.39	0.83
I-W5- 9	21.86	
I-W5-10	21.78	0.85
I-W5-11	21.62	0.83
I-W5-12	20.78	1.87
I-W5-14	20.85	0.58
I-W5-15	21.57	0.82
I-W5-16	21.61	
I-W5-17	21.07	1.67
I-W5-18	21.85	
I-W5-19	21.78	0.82
I-W5-20	21.62	0.72
I-W5-21	20.91	0.85
I-W5-22	21.51	0.78
I-W5-23	19.62	0.49
I-W5-24	20.53	0.62
I-W5-25	19.68	0.99
I-W5-26	19.92	0.53
I-W5-27	20.39	0.62
I-W5-28	19.86	0.55
I-W5-29	19.44	0.52
I-W5-30	20.00	1.43
I-W5-31	19.23	1.69
I-W5-32	20.09	0.57
I-W5-33	20.63	0.69

TABLE 1—*Continued*

NAME	V	B-V	NAME	V	B-V	NAME	V	B-V
II-W1- 1	20.72	0.74	II-W2-36	20.49	0.59	II-W4-16	21.71	0.90
II-W1- 2	21.50	0.89	II-W2-37	20.94	1.37	II-W4-17	21.84	0.63
II-W1- 3	20.76	2.04	II-W2-38	20.14	0.54	II-W4-18	19.23	0.47
II-W1- 4	21.26	0.69	II-W2-39	19.59	1.18	II-W4-19	21.34	0.89
II-W1- 5	20.83	0.64	II-W2-40	19.91	0.51	II-W4-20	20.70	0.71
II-W1- 6	21.40	1.13	II-W2-41	20.22	0.56	II-W4-21	20.72	0.74
II-W1- 7	19.53	0.54	II-W2-42	20.25	0.60	II-W4-22	20.98	1.50
II-W1- 8	19.98	0.57	II-W2-43	20.26	1.76	II-W4-23	20.87	0.73
II-W1- 9	21.57	0.71	II-W2-44	20.29	0.53	II-W4-24	21.21	0.69
II-W1-10	20.29	1.39	II-W2-45	21.35	0.84	II-W4-25	21.05	0.63
II-W1-11	20.40	0.60	II-W2-46	20.17	0.58	II-W4-26	19.40	0.49
II-W1-12	20.83	0.70	II-W2-47	21.15	0.82	II-W4-27	20.25	0.61
II-W1-13	20.45	0.62	II-W2-48	20.98	0.71	II-W4-28	20.44	0.65
II-W1-14	21.07	0.85				II-W4-29	20.68	0.68
II-W1-15	21.17	0.73				II-W4-30	21.18	0.89
II-W1-16	20.88	0.67	II-W3- 1	21.04	0.77	II-W4-31	19.60	0.51
II-W1-17	21.58	0.95	II-W3- 2	21.74	0.84	II-W4-32	21.10	0.68
II-W1-18	20.28	0.61	II-W3- 3	20.39	0.59	II-W4-33	21.54	0.72
II-W1-19	21.16	0.74	II-W3- 4	19.85	0.54	II-W4-34	20.44	0.56
II-W1-20	21.35	0.73	II-W3- 5	20.89	0.69	II-W4-35	20.86	0.68
II-W1-21	21.21	0.72	II-W3- 6	20.61	0.67	II-W4-36	21.84	
II-W1-22	20.67	0.66	II-W3- 7	21.84		II-W4-37	20.59	0.58
II-W1-23	21.03	0.65	II-W3- 8	19.87	0.54	II-W4-38	20.00	0.53
II-W1-24	19.89	0.51	II-W3- 9	21.03	0.68	II-W4-39	21.01	0.78
II-W1-25	20.57	0.69	II-W3-10	20.08	0.57	II-W4-40	20.23	0.61
II-W1-26	21.28	0.66	II-W3-11	20.55	1.71	II-W4-41	20.21	0.68
II-W1-27	21.22	0.90	II-W3-12	20.87	0.80	II-W4-42	20.04	1.68
II-W1-28	19.13	0.54	II-W3-13	21.73	0.79	II-W4-43	19.87	0.70
II-W1-29	19.62	0.51	II-W3-14	20.87	0.68			
II-W1-30	20.88	0.68	II-W3-15	20.24	0.83			
II-W1-31	20.30	0.53	II-W3-16	21.08	0.83	II-W5- 1	21.21	0.82
II-W1-32	20.43	0.58	II-W3-17	21.06	0.69	II-W5- 2	19.98	0.55
II-W1-33	21.41	0.81	II-W3-18	20.57	0.69	II-W5- 3	20.85	0.74
II-W1-34	19.13	0.48	II-W3-19	21.14	0.81	II-W5- 4	21.37	0.83
II-W1-35	19.66	0.57	II-W3-20	20.65	0.63	II-W5- 5	21.16	1.10
II-W1-36	21.26	0.79	II-W3-21	20.37	0.63	II-W5- 6	21.14	0.81
II-W1-37	21.10	0.68	II-W3-22	19.31	0.48	II-W5- 7	20.63	0.91
II-W1-38	20.22	0.63	II-W3-23	21.24	0.72	II-W5- 8	21.04	0.73
II-W1-39	20.17	0.69	II-W3-24	21.31	0.81	II-W5- 9	20.34	0.65
II-W1-40	20.84	0.68	II-W3-25	19.93	0.52	II-W5-10	21.93	
II-W1-41	19.40	0.65	II-W3-26	21.25	0.74	II-W5-11	20.59	0.86
II-W1-42	21.21	0.83	II-W3-27	20.83	0.65	II-W5-12	20.64	0.65
II-W1-43	21.09	0.76	II-W3-28	21.33	0.75	II-W5-13	20.24	1.16
			II-W3-29	21.20	0.83	II-W5-14	21.66	0.87
			II-W3-30	21.76	0.89	II-W5-15	21.83	
II-W2- 1	21.17	1.29	II-W3-31	21.47	0.78	II-W5-16	20.82	0.67
II-W2- 2	21.06	0.71	II-W3-32	20.19	0.66	II-W5-17	21.22	0.73
II-W2- 3	19.84	0.57	II-W3-33	19.94	1.30	II-W5-18	20.28	0.55
II-W2- 4	20.29	0.58	II-W3-34	20.58	0.64	II-W5-19	21.10	0.97
II-W2- 5	20.92	0.66	II-W3-35	21.04	0.67	II-W5-20	20.83	0.75
II-W2- 6	21.37	0.81	II-W3-36	20.02	0.53	II-W5-21	21.00	0.79
II-W2- 7	20.69	0.75	II-W3-37	20.57	0.64	II-W5-22	21.16	0.99
II-W2- 8	21.14	0.78	II-W3-38	20.39	1.01	II-W5-23	20.69	1.86
II-W2- 9	21.37	0.77	II-W3-39	20.92	0.72	II-W5-24	21.28	1.40
II-W2-10	21.19	0.82	II-W3-40	19.92	0.53	II-W5-25	19.68	0.52
II-W2-11	20.55	0.64	II-W3-41	20.68	0.77	II-W5-26	20.77	1.49
II-W2-12	21.26	0.63	II-W3-42	20.31	0.69	II-W5-27	20.84	0.63
II-W2-13	20.31	0.78	II-W3-43	20.39	0.57	II-W5-28	20.84	0.68
II-W2-14	20.01	0.50	II-W3-44	20.00	0.56	II-W5-29	20.97	0.74
II-W2-15	21.90	0.63	II-W3-45	19.94	0.53	II-W5-30	21.15	0.84
II-W2-16	21.16	0.77	II-W3-46	20.35	-0.15	II-W5-31	21.11	0.83
II-W2-17	21.25	0.62	II-W3-47	19.60	0.52	II-W5-32	21.28	0.78
II-W2-18	21.63	0.79				II-W5-33	21.26	0.79
II-W2-19	20.56	0.66				II-W5-34	20.85	0.73
II-W2-20	21.27	0.81				II-W5-35	21.54	
II-W2-21	20.93	0.76	II-W4- 1	21.00	0.75	II-W5-36	21.41	0.76
II-W2-22	21.85	0.77	II-W4- 2	19.60	0.46	II-W5-37	20.11	0.54
II-W2-23	21.53	0.80	II-W4- 3	21.15	0.63	II-W5-38	19.01	1.70
II-W2-24	21.79	0.75	II-W4- 4	21.78	0.56	II-W5-39	20.62	0.67
II-W2-25	21.63		II-W4- 5	21.47	0.83	II-W5-40	21.09	0.77
II-W2-26	21.14	0.88	II-W4- 6	20.52	0.87	II-W5-41	20.39	0.59
II-W2-27	21.24	0.69	II-W4- 7	20.13	0.62	II-W5-42	20.57	1.83
II-W2-28	21.09	0.75	II-W4- 8	20.86	0.66	II-W5-43	20.73	0.77
II-W2-29	21.51	0.79	II-W4- 9	20.99	0.77	II-W5-44	19.87	0.54
II-W2-30	21.28	0.78	II-W4-10	20.78	0.74	II-W5-45	20.25	0.58
II-W2-31	20.00	0.53	II-W4-11	20.75	0.80	II-W5-46	20.95	0.74
II-W2-32	19.99	0.56	II-W4-12	21.89		II-W5-47	20.18	0.56
II-W2-33	21.07	0.84	II-W4-13	19.49	0.49	II-W5-48	19.45	0.55
II-W2-34	20.35	0.57	II-W4-14	20.03	0.59	II-W5-49	19.91	0.53
II-W2-35	21.55	0.75	II-W4-15	20.84	0.71			

TABLE 2

SYSTEMATIC CORRECTIONS TO THE COLORS (FIELD ERRORS)

SECTOR	Δ(B-V)	SECTOR	Δ(B-V)
I - W1	+ 0.06	II - W1	+ 0.06
W2	+ 0.06	W2	+ 0.03
W3	+ 0.01	W3	0.00
W4	0.00	W4	0.00
W5	+ 0.03	W5	0.00

likely that an increased sample by perhaps a factor of 3 to 5 could provide the necessary statistics, if adequate accuracy in the photometry were achieved over the necessarily wider area.

III. INTRINSIC WIDTH OF THE MAIN SEQUENCE

The problem of the intrinsic width can be discussed only in a statistical sense by comparing the observed distribution about the mean (ridge) line, listed in Table 4, with the distribution of the known errors. Individual stars could truly deviate from the mean and remain undiscovered within the scatter, if the accidental errors dominate. But what can be found by deconvolving the measuring errors from Figure 1 is a *distribution* of deviants, if it is wide enough.

Certain stars must be discounted. Unresolved doubles spread the distribution asymmetrically toward the red, and stars that stand far toward the red are considered here to be foreground. It is rather obvious which stars to exclude in Figure 3, as there is a clean separation between the main-sequence distribution and the stragglers toward the red.

The distribution of the remaining stars about the ridge line is shown in Figure 3 for the same half-magnitude intervals as in Table 3. The standard deviation of the observed distribution in each interval is listed in column (2) of Table 5, and these are compared with the known measuring errors in column (3). Deconvolving columns (2) and (3) gives the formal distributions of the intrinsic width in column (4).

The solid line in Figure 3 is a Gaussian fit to the observed residuals about the ridge line, and the dashed curve is a Gaussian of the same area, using the standard deviation from the known measuring errors alone. The conclusion is that nearly all the scatter in Figure 2 is due to the accidental errors, and that the cosmic width of the main sequence could be zero. The formal widths of $\sigma(B - V) \approx \pm 0.03$ mag in the last several lines of Table 5 (col. [4]) clearly need not be taken to be significantly different from zero (Fig. 3).

IV. CHEMICAL INHOMOGENEITY OF PROTO M15

If the intrinsic width were actually zero, then the chemical composition of the member stars would all be the same because the main-sequence position depends on X and Z. What useful limits can be put on the variations of the hydrogen and heavier element contents using the present observations?

The sense of the changes in the main-sequence position caused by varying X and Z are well known. From dimensional analysis, Strömgren (1952) showed the dependence explicitly for stars on the CNO cycle with bound-free (Kramers's) opacity. Similar equations (cf. Sandage and Gratton 1963) for the p-p chain for stars with moderate metal abundance ($Z \approx 10^{-2}$) give a dependence of the approximate form

$$L \approx \text{const.}\, Z^{0.3} X^{1.5} T_e^{\,q}\,. \qquad (1)$$

However, as Z is decreased to a sufficiently low value, the bound-free opacity declines below that due to free-free H and He transitions, and the dependence of L on Z becomes even smaller. The metal abundance of M92 and M15 ($Z \approx 2 \times 10^{-4}$) is in this realm.

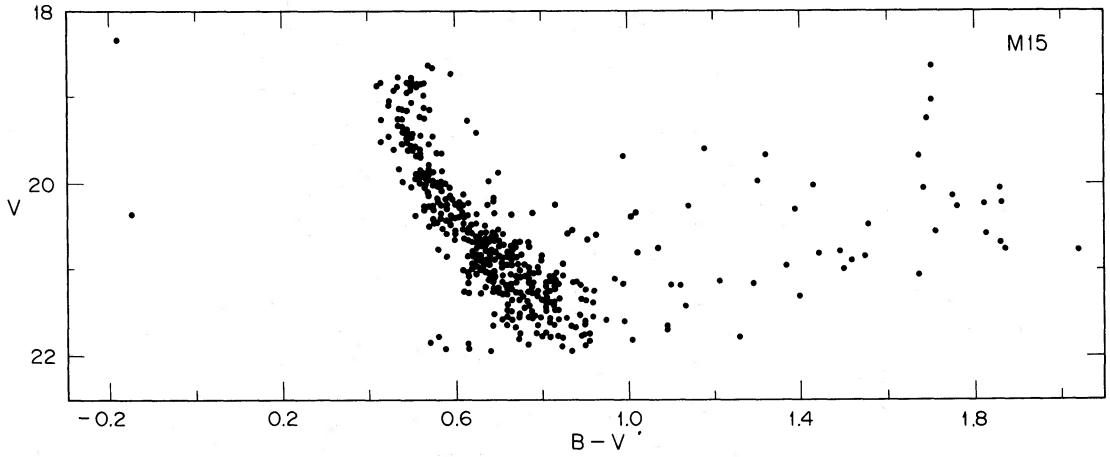

FIG. 2.—The color-magnitude diagram for the stars listed in Table 1. The points are the mean of measurements of five plates in each color.

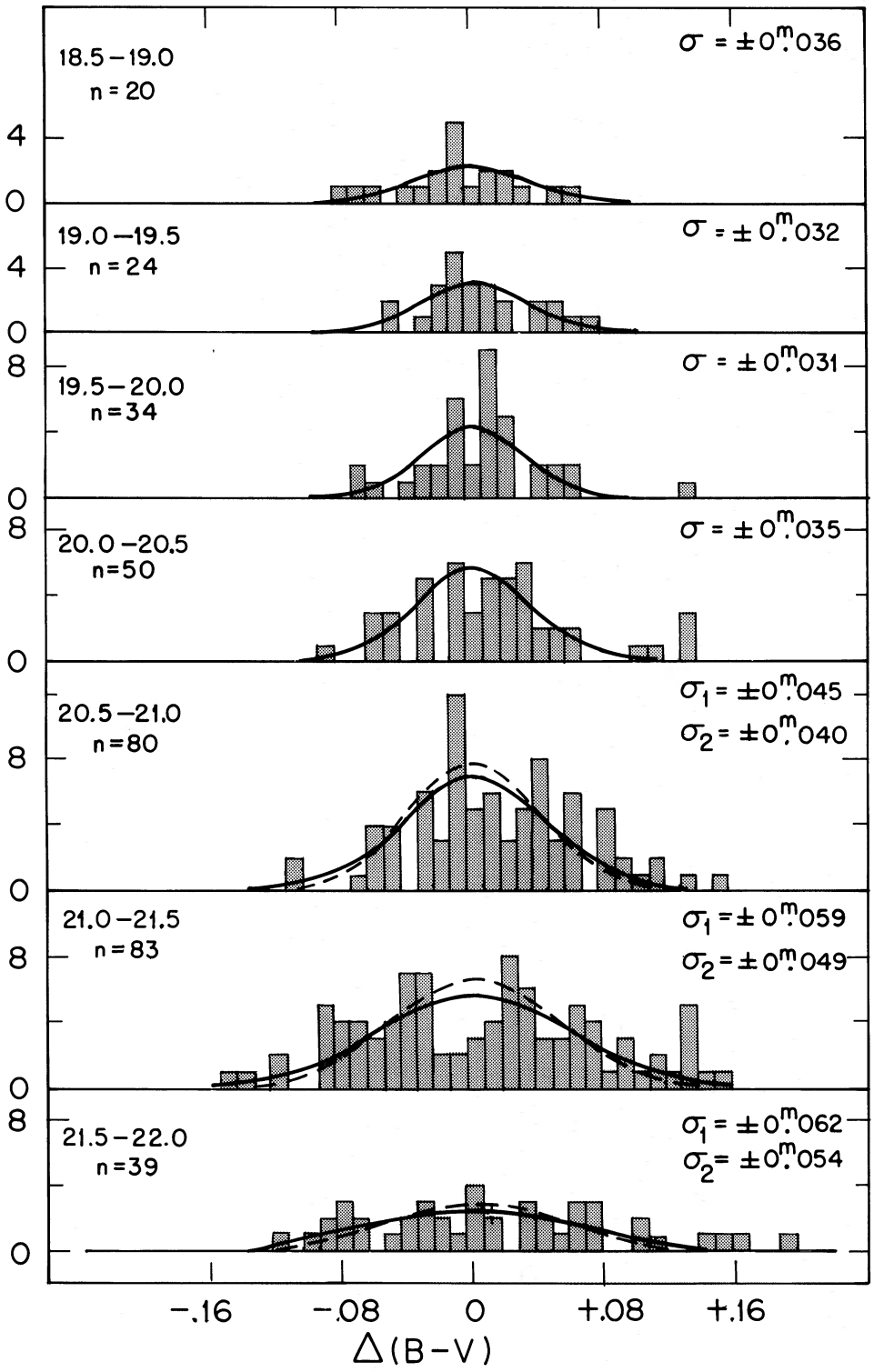

FIG. 3.—The distribution of color residuals of individual stars from the main-sequence ridge line listed in Table 4. The data are binned into half-magnitude intervals in V. The solid line is the best fitting Gaussian to the observed histograms with the same area and dispersion. The dotted lines in the last three panels are the known errors of measurement, σ_2, from Table 5. Agreement of the distributions of known errors and of the observed residuals shows that the intrinsic width of the main sequence is smaller than $\sigma[\delta(B - V)] = \pm 0.03$ mag.

TABLE 3

ERRORS OF A SINGLE MEASUREMENT*

V INTERVAL mag	σ (V) mag	σ (B) mag
18.50 - 18.99	± 0.034	± 0.032
19.00 - 19.49	0.042	0.046
19.50 - 19.99	0.046	0.042
20.00 - 20.49	0.056	0.050
20.50 - 20.99	0.061	0.053
21.00 - 21.49	0.074	0.064
21.50 - 21.99	0.083	0.068

*Five plates were measured in each color. Hence, the errors in the mean values listed in Table 1 are smaller by $\sqrt{4}$.

Iben and Rood (1970) have calculated models with four different compositions ($X = 0.7, 0.8$; $Z = 10^{-3}$, 10^{-4}), and from them a chemical dependence of

$$L \approx \text{const.}\, Z^{0.05} X^{1.8} T_e^{\,q} \qquad (2)$$

can be derived for the stated XY range. Hence, L has almost no dependence on variations in Z. However, from equation (2) and $Y \approx 1 - X$, one can put limits on permissible variations of the initial helium abundance to be

$$\delta L/L \approx 0.05\delta Z/Z - 1.8\delta Y/(1 - Y)\,. \qquad (3)$$

The present observations give an upper limit to the intrinsic scatter of $\sigma[\delta(B - V)] < \pm 0.03$ [which translates to $\sigma(\delta V) \approx \sigma(\delta L/L) < \pm 0.2$]; hence the upper limit to the helium variation is

$$\delta Y < \pm 0.08\,, \quad \text{if} \quad \langle Y \rangle = 0.3\,. \qquad (4)$$

A limit on the permissible variation of the metals of low ionization potential in the convective envelope can be put from the intrinsic width of the giant branch

TABLE 4 *

MAIN SEQUENCE RIDGE LINE

V	B-V	V_o	$(B-V)_o$
18.8	0.51	18.4	0.39
19.0	0.47	18.6	0.35
19.2	0.47	18.8	0.35
19.4	0.48	19.0	0.36
19.6	0.50	19.2	0.38
19.8	0.52	19.4	0.40
20.0	0.55	19.6	0.43
20.2	0.57	19.8	0.45
20.4	0.60	20.0	0.48
20.6	0.64	20.2	0.52
20.8	0.68	20.4	0.56
21.0	0.71	20.6	0.59
21.2	0.75	20.8	0.63
21.4	0.78	21.0	0.66
21.6	0.82	21.2	0.70
21.8	0.85	21.4	0.73
22.0	0.89	21.6	0.77

* E (B-V) = 0.12

$A_V = 0.4$

TABLE 5

OBSERVED AND INTRINSIC WIDTHS OF THE M15 MAIN SEQUENCE

INTERVAL	CM DIAGRAM OBSERVED	KNOWN ERRORS	COSMIC WIDTH
V	σ (B-V)	σ (B-V)	σ (B-V)
mag	mag	mag	mag
(1)	(2)	(3)	(4)
18.50 - 18.99....	± 0.036	± 0.023	± 0.028
19.00 - 19.49....	± 0.032	± 0.031	± 0.008
19.50 - 19.99....	± 0.031	± 0.031	± 0.000
20.00 - 20.49....	± 0.035	± 0.038	± 0.000
20.50 - 20.99....	± 0.045	± 0.040	± 0.021
21.00 - 21.49....	± 0.059	± 0.049	± 0.032
21.50 - 21.99....	± 0.062	± 0.054	± 0.030

at the level of the horizontal branch. The reddening-free color $(B - V)_{0,g}$ of the ridge line of the giant sequence at this magnitude is well correlated with metal abundance (Sandage and Smith 1966). Additional southern clusters that add to the correlation are given by Cannon (1974).

Model calculations by Demarque and Geisler (1963) and by Rood (1972, Fig. 1), and observations of $R - I$ colors by Eggen (1972, Fig. 11) show that the redward shift of the giant branches that occurs when (Fe/H) increases is primarily a change in the Hayashi track in the (L, T_e)-plane. Some blanketing, in addition, is, of course, involved to enhance the effect in $B - V$ diagrams (cf. Bell and Gustafsson 1975).

Butler's (1975) calibration (see also Norris and Bessell 1975) gives

$$\log (\text{Fe/H}) = 7.2(B - V)_{0,g} - 7.0 + \log (\text{Fe/H})_\odot\,. \qquad (5)$$

The cause is evidently related to the change in the opacity of the outer convective envelope as the chemical composition is changed. This opacity controls the size of the envelope, hence the radius, and therefore the position of the Hayashi track. The chemical elements involved are those of low ionization potential such as Fe and Ca, and hence the argument here pertains strictly to the abundances of them alone.[1] However, if we assume that the *relative* abundances of all elements heavier than helium remain constant, then the surface abundance which Butler has measured relates directly to the interior Z, and

$$\sigma(\delta Z/Z) = 16.5\sigma[\delta(B - V)]\,. \qquad (6)$$

The intrinsic width of the giant branch in M15 is observed to be less than $\sigma[\delta(B - V)] = 0.01$ mag (Sandage, Katem, and Kristian 1968), hence

$$\sigma(\delta Z/Z) < \pm 0.16\,, \qquad (7)$$

which is a remarkably small limit.

[1] We are indebted to Pierre Demarque for this comment.

TABLE 6

DIFFERENTIAL LUMINOSITY FUNCTION FOR SECTORS I AND II *

V	I φ (V)	II φ (V)	I + II φ (V)	Complete I + II φ (V)
18.75 - 18.99....	3 (2)	7 (1)	10 (3)	13
19.00 - 19.24....	4 (4)	4 (1)	8 (5)	13
19.25 - 19.49....	2	10	12	12
19.50 - 19.74....	8 (2)	8 (5)	16 (7)	23
19.75 - 19.99....	5	14	19	19
20.00 - 20.24....	5 (5)	18	23 (5)	28
20.25 - 20.49....	10 (2)	23	33 (2)	35
20.50 - 20.74....	19 (1)	23	42 (1)	43
20.75 - 20.99....	19	28 (2)	47 (2)	49
21.00 - 21.24....	12 (1)	43 (8)	55 (9)	64
21.25 - 21.49....	15 (6)	23 (16)	38 (22)	60
21.50 - 21.74....	20 (13)	13 (16)	33 (29)	62
Total	122 (36)	214 (49)	336	
	158	263	421	421

* Area of sector I is 11.5 □′
Area of sector II is 10.5 □′

It should again be emphasized that a few individual stars could be chemically inhomogeneous to limits well beyond those of equations (4) and (7) and be hidden in the scatter, but a substantial fraction cannot have inhomogeneities that are much beyond these values.

The results suggest that the M15 protocloud was not enriched progressively during its collapse, otherwise these rather narrow limits to any interior chemical inhomogeneities would not exist.

V. LUMINOSITY FUNCTION TO $M_V \approx +6.5$

Most of the stars in the bins of Figure 1 were measured, and are listed in Table 1. However, later inspection showed that some stars were not marked. The magnitudes of these were estimated and were added to the sums to produce a differential luminosity function for sectors I and II, listed in Table 6 and shown in Figure 4. The numbers in parentheses and the open bars in Figure 4 are these stars added by visual inspection.

The steep rise in $\varphi(M)$ between $M_V \approx +3.5$ to $+5.5$ is expected, and it has a slope of $S \equiv d \log \varphi(V)/dV \approx +0.35$, which is similar to that in M92 with $S = +0.31$ over the same interval (Hartwick 1970; van den Bergh 1975), which also is the same as the van Rhijn function for the solar neighborhood, again over the same interval.

The situation may be different in M3 where the available data show the slope to be $S \approx 0.4$ between $M_V = +3$ to 4.5, from which it continuously declines between $M_V = +4.5$ and $+7$ to a value near $S = 0.1$ at $M_V = +7$ (Sandage 1975*a*, Table 9), but, as stated in § I, the M3 work should be repeated.

The most interesting aspect of the current data for M15 is the leveling off of $\varphi(M)$ in the last three intervals fainter than $V = 21$ ($M_V > 5.7$), similar to van den Bergh's (1975) new result in M92. Inspection of the plates leads us to believe that we cannot have missed the stars necessary to keep $\varphi(V)$ growing at the rate it has in the interval $+4 < M_V < +5.5$; hence we conclude that they are not there, at least in sectors I and II. However, despite this, the data are so near the plate limit at $V \approx 22$ that we are not totally convinced of the result, and we hope to test it using deeper plates taken on the new IIIa-J and 127-04 fine-grain plates.

VI. DENSITY FUNCTION FOR FIELD DWARFS

Nearly all of the stars (Fig. 2) redward of the main sequence must be foreground dwarfs. However, to

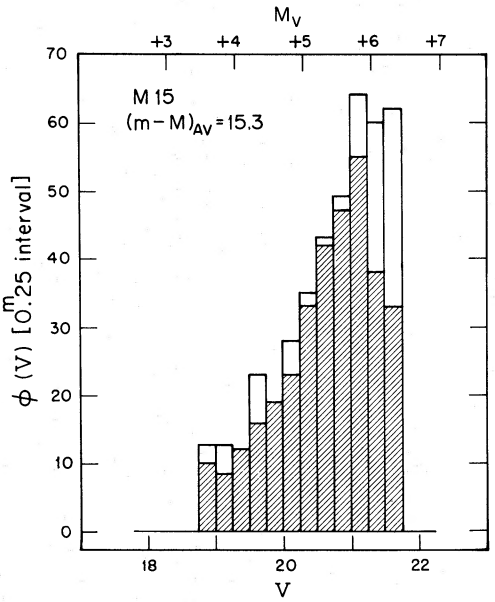

FIG. 4.—The differential luminosity function in sectors I and II, binned in 0.25 mag intervals. The shaded histograms show the sums from Table 1. The open bars are additions of stars not marked in these sectors but found from visual inspection of the plates.

estimate the numbers that are expected between $V = 19$ and 22 in the 0.0061 square degree area requires calculation from stellar statistics, because observational data on star counts in random fields at this faint level are sparse.

Because the stars are dwarfs, we can restrict the calculation to the main sequence fainter than $M_V = +8$ by counting the numbers redward of $(B - V)_0 = 1.4$ (cf. the color-magnitude diagrams for nearby dwarfs by Sandage 1957*b*, or Woolley *et al.* 1970, Fig. 2, for example).

Integration of

$$A(m_V) = 1.86 \times 10^{-6} \int_{M_V=+8}^{\infty} r^2 \varphi(M_V) D(r) dr \quad (8)$$

provides the number of stars in the area redder than $(B - V)_0 = 1.4$ between $m - \frac{1}{2}$ and $m + \frac{1}{2}$, where the magnitudes and distances are related by $m = M + 5 \log r - 5$ in the absence of absorption, $\varphi(M_V)$ is the differential luminosity function, $D(r)$ is the density function normalized to 1 at $r = 0$, and the factor before the integral sign is the fraction of the entire sphere (times 4π) in the area of 22 arcmin^2 (0.0061 square degrees).

The requirement is to produce the observed $A(m)$ values of $A(19) = 3$, $A(20) = 8$, and $A(21) \approx 16$ (the last is corrected for a factor of ~ 2 incompleteness due to the plate limit at $B \approx 23$) for stars redder than $B - V = 1.5$ [i.e., using $E(B - V) = 0.1$ mag], using appropriate $\varphi(M_V)$ and $D(r)$ distributions. But what is appropriate? Since we can only determine the product $\varphi(M_V)D(r)$ from equation (8), the solution from counts alone is not unique, and the problem must be modeled.

The two principal possibilities are: (1) The stars are all of the disk population, whose luminosity distribution is van Rhijn–like, normalized to the number of stars per pc^3 in the solar neighborhood (e.g., McCuskey 1966, Table 8), and with a density gradient perpendicular to the galactic plane that applies to the disk population (i.e., $d \log D(z)/dz \lesssim -1$, z in kpc, following Weistrop 1972*b*, for example). (2) The stars are dwarfs of the halo population. In this case the density of *disk* stars at the relevant heights that contribute to the faint $A(m)$ values would be so low (due to a very high density gradient) as to be negligible, leaving only the halo contribution.

We can test these two models, or any combination of them, by calculating the number of disk stars expected at each height, using an appropriate density gradient perpendicular to the plane, combined with the absolute number of such stars in the plane at the solar neighborhood (i.e., the van Rhijn luminosity function). These numbers can then be compared with the expected number of halo dwarfs at the same heights, calculated from the known number of RR Lyrae stars as a function of z and an assumed ratio of Population II dwarfs to RR Lyrae stars, to test if halo or disk stars dominate the counts.

To start the self-consistent procedure we first calculate the required density gradient for disk-like stars that will produce the observed $A(m)$'s in Figure 2.

Various $D(z)$ functions were used, taken from two modern studies of the north galactic pole by Fenkart (1967, 1969) and Becker (1970), and by Weistrop (1972*b*) in SA 57. Equation (8) was solved by the m, $\log \pi$ method of Kapteyn (e.g., Bok 1937, Table 9), using the trial polar gradients on the assumption that the density at distance r in the M15 field at latitude $b = -27°$ was equal to the SA 57 value at $z = r \sin b$. The van Rhijn $\varphi(M)$ was used as normalized by McCuskey (1966, Table 8) at the position of the Sun.

The result is that the observed $A(m)$ values can only be reproduced with a steep density gradient of $\log D(z) = -1.1\, z$ (z in kpc), which gives $A(19) = 6$, $A(20) = 10$, and $A(21) = 15$, from equation (8), in reasonable agreement with the observed values of 3, 8, and 16. The disk gradients obtained by Fenkart for brighter stars than we are considering here (i.e., $M_G = +3$ to $+8$) are $d \log D(z)/dz = -0.55$ in the average, and -0.83 as his steepest. Both predict too many stars, the first by a factor of 4, and the second by a factor of 2 throughout the interval from $B = 19$ to 21. Our required gradient of -1.1 agrees with Weistrop's (1972*b*, her Fig. 5) for her faint dwarfs, if we restrict her analysis to $z \geqslant 300$ pc.

Suppose now that the second model applies where the true disk gradient is much steeper than -1.1 so that no disk stars are involved at the relevant heights, in which case all observed field stars in Figure 2 would be halo dwarfs. What normalized $\varphi(M)$ is then required to produce the observed $A(m)$'s?

The appropriate density gradient for the Population II halo dwarfs is that which applies to the RR Lyrae stars, and it is known that this is extraordinarily shallow compared with the gradient for disk stars. The modern work on the RR Lyrae gradient from the Lick survey (Kinman, Wirtanen, and Janes 1966) and from the Palomar-Gronigen survey (Plaut 1970) agrees with the earlier work by Perek (1951) and the rediscussion by Plaut and Soudan (1963) in showing that the gradient of halo stars lies between $d \log D(z)/dz = -0.07$ and -0.3 (z in kpc).

Suppose that we apply a gradient of -0.2 to the main-sequence dwarfs, and use a $\varphi(M)$ that again has the van Rhijn normalization at the Sun. Equation (8) for this case, again for stars with $+8 \leq M_V \leq +12$, gives the values $A(17) = 7$, $A(18) = 25$, $A(19) = 81$, $A(20) = 230$, and $A(21) = 558$ in an area of 0.041 square degrees (the same as Becker's 1970 photometry) at the galactic pole. Becker's counted numbers (his Fig. 3) are $A(17) = 0$, $A(18) = 2$, $A(19) = 3$, $A(20) = 7$, and $A(21) \approx 10$, which are a factor of ~ 30 times smaller. Hence, if the stars in Figure 2 were in fact halo stars, then the ratio of disk to halo dwarfs at the Sun would have to be 30 to 1 to explain the counts. But this ratio gives far too many Population II stars in the plane. For example, Schmidt's (1976) estimate, based on statistics of local high velocity stars, is 1000 to 1. Hence, because the true ratio of disks to halo dwarfs is much greater than 30 to 1, the conclusion is that the halo stars

TABLE 7

PREDICTED AND OBSERVED COUNTS IN 0.042 □° AT THE GALACTIC POLE FOR VARIOUS ASSUMED DENSITY GRADIENTS USING THE VAN RHIJN φ(M) NORMALIZED TO THE SOLAR NEIGHBORHOOD

GRADIENT	APPARENT VISUAL MAGNITUDE					
d LOG D(z)/d(z)	17	18	19	20	21	22
	A (m_V)					
- 0.20....	7	25	81	230	558	1085
- 0.55....	5	13	31	57	85	108
- 0.83....	4	8	16	24	31	36
- 1.1.....	3	5	9	12	15	17
- 1.4.....	2	3	5	7	8	8
OBSERVED	0	2	3	7	~10	-

that are at the heights which contribute to the counts between $V = 18$ and 22 are far too few to add appreciably to the observed numbers.

Another less certain way to the same conclusion is a consistency test of the disk model. Here we again assume that the observed stars are disk population, and show that the number of disk dwarfs at the heights which contribute to the counts is, in fact, larger than the halo contribution.

Consider Becker's counts in SA 57. If his faint dwarfs are disk population, what density gradient is needed to produce the counts? The results of solving equation 8 on the assumption of a van Rhijn $\varphi(M)$ normalized to the solar neighborhood are given in Table 7, which shows that a gradient of -1.4 will satisfy the observations.

The next step is to inspect the $(m, \log \pi)$-table for this solution. The entries show that there are $\sim 2 \times 10^4$ dwarfs per cubic kpc in the absolute magnitude interval $M_V = 7.5$ to 8.5 at a height of $z = 1585$ pc (they appear in the apparent magnitude interval $V = 18.5$ to 19.5). The number has dropped to $\sim 10^3$ per kpc at $z = 2512$ pc (note the steep decay).

If the disk model is correct, then the number of halo dwarfs at these same heights must be smaller than these numbers. The only moderately certain datum on the halo numbers at these heights is the absolute density of RR Lyrae stars. Kinman, Wirtanen, and Janes, together with Perek and with Plaut and Soudan, put the density of RR Lyraes of Bailey type *ab* at ~ 3 per kpc^3 at $z = 1.5$ kpc in the direction of the pole. We now suppose that the *halo population* has the same ratio of dwarfs to RR Lyrae stars as in the globular cluster M3 (i.e., ~ 200 RR Lyrae stars to $\sim 5 \times 10^4$ main-sequence dwarfs between $M_V = 7.5$ and 8.5, from Sandage 1957, Table 9, using the $\varphi[M]$ there, multiplied by 5 to change to a 1 mag interval and by 2.5 to account for the increase from $\varphi[6]$ to $\varphi[8]$ at a rate of $d \log \varphi[M]/dM = 0.2$). Hence, the ratio in M3 is 1 RR Lyrae to ~ 250 dwarfs between $M_V = +7.5$ and $+8.5$.

Consequently, with three RR Lyrae stars per kpc^3 at $z \approx 1.5$ kpc, the number of *Population II main-sequence progenitors* of the M3 type (between $M_V =$ 7.5 and 8.5) would be ~ 750 per kpc^3 at this height, which is a factor of 25 smaller than the 2×10^4 disk dwarfs per kpc^3 at $z = 1.6$ kpc, and is about equal to the number at $z = 2.5$ kpc. Hence, we have a large margin of safety in the disk model even if the ratio of Population II dwarfs to RR Lyrae stars were considerably larger than the M3 case. (Note that those stars of absolute magnitude $+10$ that are at a height of $z = 2.5$ kpc have apparent magnitude $V = 22$.)

Our conclusion is then that the halo and the disk population coexist at $z \approx 2$ kpc, that the red stars seen in Figure 2 and in Becker's (1970) SA 57 diagram (his Fig. 2) are disk stars with $d \log D(z)/dz \approx -1.4$, and that although the true halo Population II main sequence is present (as required to produce the RR Lyrae stars), it is too weak to contribute to the counts for $B - V > 1.4$ brighter than $V = 22$. The disk and halo densities apparently become equal at about $z \approx 2.5$ kpc, above which the halo population rapidly dominates. However, the value for the transition height is uncertain from our data, since it depends here on the highly variable mean ratio of the number of RR Lyrae variables to main-sequence progenitors.[2]

The evidence for coexistence of the two populations at these heights is of the most straightforward kind. The numbers of red stars fainter than $V = 19$ in two areas (M15 and SA 57) are so small as to require very steep density gradients if the objects are disk stars. Conversely, the numbers are much too large to be halo stars, if one uses any reasonable absolute normalization of the halo density at the Sun. The disk gradient that is required to satisfy the observations is so much steeper than the well-established halo gradient

[2] The uncertainty of this discussion, of course, is that the normalized number of RR Lyrae stars to main-sequence dwarfs varies greatly from cluster to cluster, and the M3 ratio may not be representative of the field, but rather may represent an extreme of the distribution. But, as mentioned in the text, the disk model would still apply even if the actual ratio of dwarfs to RR Lyrae stars were ~ 25 times greater than in M3. And because the calculation as given agrees with the estimates by Schmidt, obtained differently, we accept the conclusion: see n. 3.

(for RR Lyrae stars) that it shows the coexistence of the two populations directly.[3]

Several avenues for future work seem open on the problem. High proper-motion stars can be studied to test if the number of high W-velocity halo red dwarfs that are passing through the solar neighborhood is in the proper ratio to the known number of brighter (local) halo subdwarfs ($4 \leq M_V < 8$) per unit volume. The number of such subdwarfs close to the plane between $V \approx 10$ and 12 can be found from photometric studies of complete proper-motion samples (such as the Bruce Proper Motion Survey by Luyten and the Lowell survey by Giclas and his collaborators). If similar completeness for the high-velocity M dwarfs could be achieved between $V \approx 14$ and 16 (4 mag fainter), this ratio could be found, leading directly to some idea of the halo Population II $\varphi(M)$. Work on the bright end of $\varphi(M)$ along these lines has begun by Eggen (cf. 1974) and by Rodgers and Eggen (1974), and studies are nearly complete for a number of the northern Lowell proper-motion fields (Sandage and Kowal 1977).

A deep sampling survey in B, V, and R magnitudes of the halo from $V = 17$ to $V = 23$ could give the population characteristics directly by standard statistical methods. The Basel program (cf. Becker 1972) has been especially valuable for stars brighter than $V \approx 18$. Work on a new deep survey using the new generation of wide field large reflectors has recently been started here to carry the work to faint limits near $V \approx 23$.

Such projects on the halo density and luminosity functions, and on the apparently well-established gradient of chemical composition within the halo itself, promise to aid in the present attempts to reconstruct the historical Galactic collapse.

[3] If the two populations have equal density at $z = 2.5$ kpc, and if the disk has a gradient of -1.4 while the halo has -0.2, then the disk stars will outnumber the halo stars at $z = 0$ (i.e., at the position of the Sun in the plane) by 1000 to 1, in agreement with Schmidt (1975) and Weistrop (1972*a*), showing the consistency of our model with Schmidt's estimate of the population ratio in the plane.

VII. CONCLUSIONS

1. Results of the photometry of ~ 350 stars fainter than $V \approx 19$ near M15 show a main sequence whose observed width is due almost entirely to the errors of measurement. This, together with the narrowness of the subgiant branch, puts significant limits on any initial chemical inhomogeneity that could have been present at the end of the collapse phase of proto M15.

2. The luminosity function of M15 at $M_V \approx +6$ may have a change of slope, in the sense of fewer stars per magnitude interval at fainter levels.

3. The density gradient of main-sequence red dwarfs in the range $+8 \lesssim M_V \lesssim +12$ must be as steep as $d \log D(z)/dz \approx -1.4$ per kpc to explain the very few numbers of stars redder than $B - V = 1.4$ observed in both the M15 foreground and in the north galactic pole region of SA 57. This is *much* steeper than the RR Lyrae gradient of ~ -0.2 dex per kpc, and in combination with other data shows that the bulk of the red main-sequence stars at $z \approx 2$ kpc are not progenitors of the RR Lyrae stars, but rather are extensions of the disk. The extreme Population II halo main-sequence stars that do evolve into the RR Lyrae stars must have a lower number density at $z \approx 2$ kpc than these disk stars, otherwise more field stars would be observed in the interval $19 < V \lesssim 22$.

We wish to thank an anonymous referee for correcting an error in the original version of § IV, and for other helpful suggestions. We are also indebted to Pierre Demarque for important comments on parts of the manuscript.

REFERENCES

Aizenman, M. L., Demarque, P., and Miller, R. H. 1969, *Ap. J.*, **155**, 973.
Becker, W. 1960, *Astr. Ap.*, **9**, 204.
———. 1972, *Quart. J.R.A.S.*, **13**, 226.
Bell, R. A., and Gustafsson, B. 1975, *Dudley Obs. Report*, No. 9, p. 319.
Bessell, M. S., and Norris, J. 1976, *Ap. J.*, **208**, 369.
Bok, B. J. 1937, *Distribution of Stars in Space* (Chicago: University of Chicago Press), p. 28.
Butler, D. 1975, *Pub. A.S.P.*, **87**, 559.
———. 1976, Report at August 1976 Tucson Workshop for Southern Hemisphere Problems (unpublished).
Cannon, R. D. 1974, *M.N.R.A.S.*, **167**, 551.
Cannon, R. D., and Stobie, R. S. 1973, *M.N.R.A.S.*, **162**, 207.
Demarque, P., and Geisler, J. E. 1963, *Ap. J.*, **137**, 1102.
Eggen, O. J. 1972, *Ap. J.*, **172**, 639.
———. 1974, *Pub. A.S.P.*, **86**, 697.
Eggen, O. J., and Sandage, A. 1969, *Ap. J.*, **158**, 669.
Fenkart, R. P. 1967, *Zs. Ap.*, **66**, 390.
———. 1969, *Astr. Ap.*, **3**, 228.
Freeman, K. C., and Rodgers, A. W. 1975, *Ap. J.* (*Letters*), **201**, L71.
Geyer, E. H. 1967, *Zs. Ap.*, **66**, 16.
Hartwick, F. D. A. 1970, *Ap. J.*, **161**, 845.
Iben, I., and Rood, R. T. 1970, *Ap. J.*, **159**, 605.
Kinman, T. D., Wirtanen, C. A., and Janes, K. A. 1966, *Ap. J. Suppl.*, **13**, 379.
Mallia, E. A. 1975, *M.N.R.A.S.*, **170**, 57P.
———. 1976, *Astr. Ap.*, **48**, 129.
McCuskey, S. W. 1966, in *Vistas in Astronomy*, Vol. **7**, ed. A. Beer (New York: Pergamon Press), p. 141.
Norris, J., and Bessell, M. S. 1975, *Ap. J.* (*Letters*), **201**, L75.
Norris, J., and Zinn, R. 1976, private communication.
Perek, L. 1951, *Contr. Astr. Inst. Brno*, Vol. **1**, No. 8.
Plaut, L. 1970, *Astr. Ap.*, **8**, 341.
Plaut, L., and Soudan, A. 1963, *B.A.N.*, **17**, 70.
Rodgers, A. W., and Eggen, O. J. 1974, *Pub. A.S.P.*, **86**, 742.
Rood, R. T. 1972, *Ap. J.*, **177**, 681.
Sandage, A. 1954, *A.J.*, **59**, 162.
———. 1957*a*, *Ap. J.*, **125**, 422.
———. 1957*b*, in *Stellar Populations*, ed. D. O'Connell (Vatican City: Specola Vaticana), Vol. **5**, p. 286.
———. 1970, *Ap. J.*, **162**, 841.
Sandage, A., and Gratton, L. 1963, *Star Evolution* (New York: Academic Press), p. 11.
Sandage, A., Katem, B., and Kristian, J. 1968, *Ap. J.* (*Letters*), **153**, L129.
Sandage, A., and Kowal, C. T. 1977, in preparation.
Sandage, A., and Smith, L. L. 1966, *Ap. J.*, **144**, 886.
Schmidt, M. 1975, *Ap. J.*, **202**, 22.

Strömgren, B. 1952, *A.J.*, **57**, 65.
van den Bergh, S. 1975, *Ap. J.*, **201**, 585.
Weistrop, D. 1972*a*, *A.J.*, **77**, 366.
———. 1972*b*, *A.J.*, **77**, 849.
Woolley, R., Epps, E. A., Penston, M. J., and Pocock, S. B. 1970, *Roy. Obs. Ann.*, No. 5.
Zinn, R. 1973*a*, *Astr. Ap.*, **25**, 409.
———. 1973*b*, *Ap. J.*, **182**, 183.

BASIL KATEM and ALLAN SANDAGE: Hale Observatories, 813 Santa Barbara Street, Pasadena, CA 91101

PLATE 4

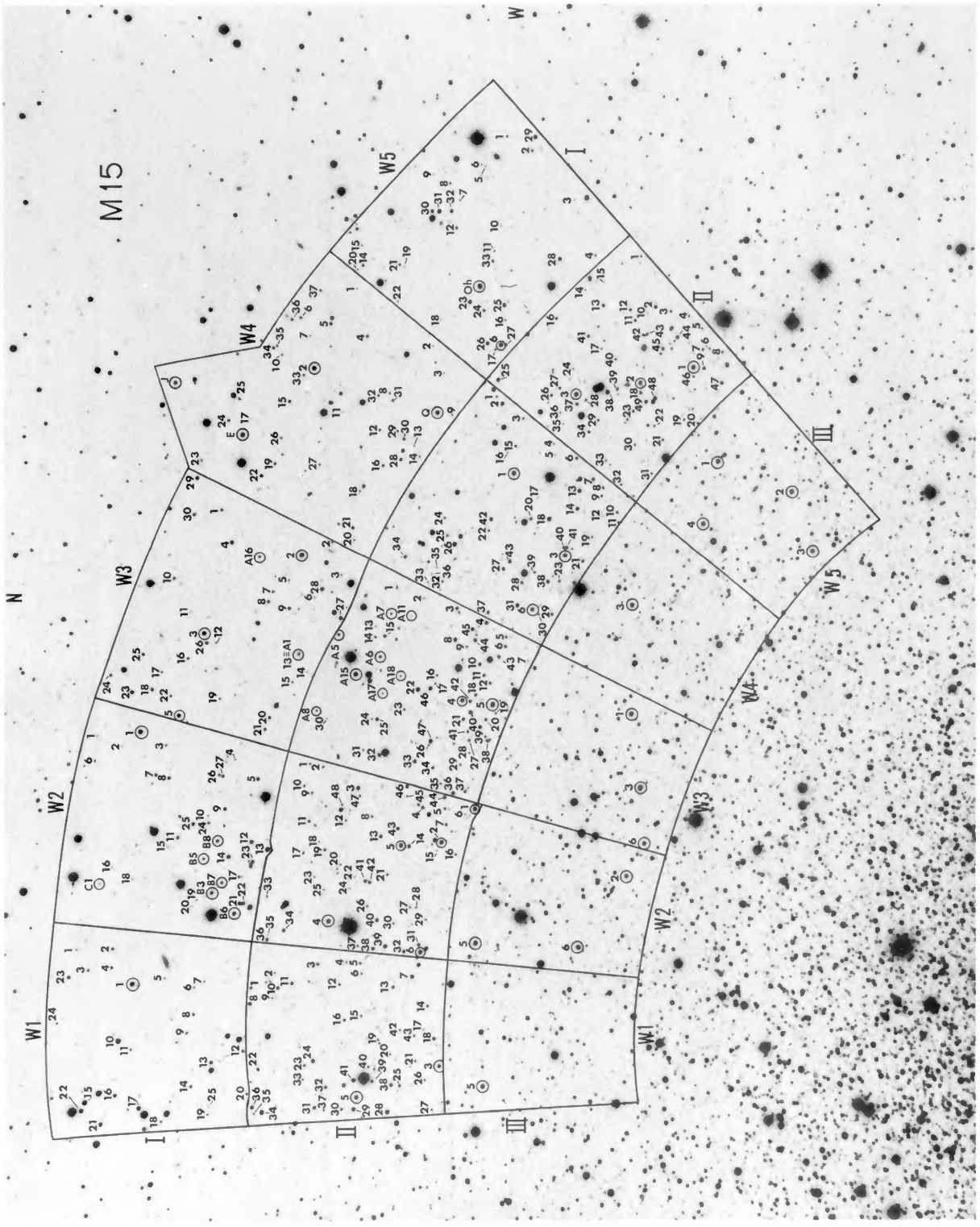

FIG. 1.—Identification chart for the M15 program stars listed in Table 1. The photoelectric standards are circled. The area is about 8′ north and slightly west of the cluster center. Reproduction is from a 50 min exposure with Eastman 103a-D emulsion behind a Schott GG11 filter taken with the Hale 5 m reflector.